

Unbiased Cosmic Opacity Constraints from Standard Sirens and Candles

JUN-JIE WEI^{1,2}

¹*Purple Mountain Observatory, Chinese Academy of Sciences, Nanjing 210034, China*

²*Guangxi Key Laboratory for Relativistic Astrophysics, Guangxi University, Nanning 530004, China*

ABSTRACT

The observation of Type Ia supernovae (SNe Ia) plays an essential role in probing the expansion history of the universe. But the possible presence of cosmic opacity can degrade the quality of SNe Ia. The gravitational-wave (GW) standard sirens, produced by the coalescence of double neutron stars and black hole–neutron star binaries, provide an independent way to measure the distances of GW sources, which are not affected by cosmic opacity. In this paper, we first propose that combining the GW observations of third-generation GW detectors with SN Ia data in similar redshift ranges offers a novel and model-independent method to constrain cosmic opacity. Through Monte Carlo simulations, we find that one can constrain the cosmic opacity parameter κ with an accuracy of $\sigma_\kappa \sim 0.046$ by comparing the distances from 100 simulated GW events and 1048 current Pantheon SNe Ia. The uncertainty of κ can be further reduced to ~ 0.026 if 800 GW events are considered. We also demonstrate that combining 2000 simulated SNe Ia and 1000 simulated GW events could result in much severer constraints on the transparent universe, for which $\kappa = 0.0000 \pm 0.0044$. Compared to previous opacity constraints involving distances from other cosmic probes, our method using GW standard sirens and SN Ia standard candles at least achieves competitive results.

Keywords: cosmology: observations — distance scale — gravitational waves — supernovae: general

1. INTRODUCTION

In 1998, the accelerated expansion of the universe was first revealed by the unexpected dimming of Type Ia supernovae (SNe Ia) (Riess et al. 1998; Perlmutter et al. 1999). Soon after the discovery of cosmic acceleration, a cosmological distribution of dust has been suggested as an alternative explanation for the observed dimming of SNe Ia (Aguirre 1999a,b). Indeed, SN observations are affected by dust in the Milky Way, the intergalactic medium, intervening galaxies, and their host galaxies. The extinction effects of SNe Ia caused by these dust in the Milky Way and their host galaxies have been well modeled and they have no impact on the conclusion of cosmic acceleration. However, cosmic opacity may also be due to other exotic mechanisms, in which extragalactic magnetic fields turn photons into unobserved particles (e.g., light axions, gravitons, chameleons, Kaluza-Klein modes) (Chen 1995; Deffayet & Uzan 2000; Csáki et al. 2002; Khoury & Weltman 2004; Burrage 2008; Avgoustidis et al. 2010; Jaeckel & Ringwald 2010). We have little knowledge about exotic mechanisms for cosmic opacity

and their influence on SN observations. Therefore, the question of whether cosmic opacity can be responsible for part of the dimming of standard candles remains open. As more than 1000 SNe Ia have been detected (Scolnic et al. 2018), their cosmological constraint ability is now limited by systematic uncertainties rather than by statistical errors. An important systematic uncertainty is the mapping of cosmic opacity. In the era of precision cosmology, it is necessary to accurately quantify the transparency of the universe.

In the past, the cosmic distance duality (CDD) relation has been used to verify the presence of opacity and systematic uncertainties in SN Ia data. The luminosity distance (D_L) and the angular diameter distance (D_A) are related by the CDD relation (Etherington 1933; Ellis 2007): $D_L = D_A(1+z)^2$. This relation holds for all cosmological models described by Riemannian geometry, requiring that photons travel along null geodesics and the number of photons is conserved (Ellis 2007). Many works have been performed to test the validity of the CDD relation (e.g., Bassett & Kunz 2004; Uzan et al. 2004; Holanda et al. 2010, 2011, 2012; Khedekar & Chakraborti 2011; Li et al. 2011; Nair et al. 2011; Gonçalves et al. 2012; Meng et al. 2012; Ellis et al. 2013; Yang et al. 2013; Liao et al. 2016; Lv & Xia 2016; Rana et al. 2016; Yang et al. 2017; Hu & Wang 2018; Lin et al. 2018a; Ma & Corasaniti 2018; Melia 2018; Ruan et al.

2018). Meanwhile, assuming the deviation from the CDD relation is attributed to the non-conservation of photon number, the opacity of the universe has been widely tested with astronomical observations (e.g., Avgoustidis et al. 2009, 2010; More et al. 2009; Lima et al. 2011; Chen et al. 2012; Nair et al. 2012; Holanda et al. 2013; Li et al. 2013; Liao et al. 2013, 2015; Holanda & Busti 2014; Hu et al. 2017; Jesus et al. 2017; Wang et al. 2017). In these works, some tests of cosmic opacity were carried out by adopting specific cosmological models and others were given in a model-independent way. There are two general methods to obtain model-independent constraints on cosmic opacity. The first is to confront the luminosity distances inferred from SN Ia observations with the opacity-independent angular diameter distances derived from baryon acoustic oscillations or galaxy clusters (More et al. 2009; Chen et al. 2012; Nair et al. 2012; Li et al. 2013). The other model-independent method was proposed by comparing the luminosity distances of SNe Ia with the opacity-free luminosity distances obtained from the Hubble parameter $H(z)$ or the ages of old passive galaxies (Holanda et al. 2013; Liao et al. 2013, 2015; Jesus et al. 2017; Wang et al. 2017).

On the other hand, because the waveform signals of gravitational waves (GWs) from inspiralling and merging compact binaries encode D_L information (Schutz 1986), one may construct the $D_L - z$ relation to probe cosmology if their electromagnetic (EM) counterparts with known redshifts can be detected (see also Holz & Hughes 2005; Messinger et al. 2014; Zhao & Wen 2018). GWs are therefore deemed as standard sirens, analogous to SN Ia standard candles. Recently, the detection of the GW event GW170817 coincident with its EM counterparts from a binary neutron star (NS) merger provided a standard-siren measurement of the Hubble constant H_0 (Abbott et al. 2017). In addition to measuring H_0 , other cosmological applications of future GW data have also been explored, such as constraining the cosmological parameters and the nature of dark energy (e.g., Holz & Hughes 2005; Zhao et al. 2011; Del Pozzo 2012; Cai & Yang 2017; Del Pozzo et al. 2017; Du et al. 2018; Wei et al. 2018), probing the CDD relation (Yang et al. 2017), testing the anisotropy of the universe (Cai et al. 2018; Lin et al. 2018b), weighing the total neutrino mass (Wang et al. 2018), estimating the time variation of Newton’s constant G (Zhao et al. 2018), and determining the cosmic curvature in a model-independent way (Wei 2018).

Unlike the distance calibrations of SNe Ia that are affected by cosmic opacity, distance measurements from GW observations have the advantage of being insensitive to the non-conservation of photon number. Therefore, GW standard sirens provide a novel way to determine the opacity-independent D_L of SNe Ia at the same redshifts. In this paper, we first propose that unbiased cosmic opacity tests can

be performed by combining SN Ia and GW data in similar redshift ranges. We make a detailed research on what level of opacity constraints may be achieved using future GW observations from the third-generation GW detectors such as the Einstein Telescope (ET).

The rest of the paper is organized as follows. In Section 2, we describe the opacity dependence of SN standard candles. In Section 3, we give an overview of using GWs as standard sirens in the potential ET observations. Unbiased cosmic opacity constraints from standard sirens and candles are discussed in Section 4. Finally, conclusions are drawn in Section 5. Throughout we use the geometric unit $G = c = 1$.

2. OPACITY DEPENDENCE OF SNE IA

As pointed out by Avgoustidis et al. (2009), the distance moduli derived from SNe Ia would be systematically influenced if there was a source of “photon absorption” affecting the universe transparency. Any effect reducing the photon number would dim the SN luminosity and increase its D_L . If $\tau(z)$ represents the opacity from a source at z to an observer at $z = 0$ due to extinction, the received flux from the source would be decreased by a factor $e^{-\tau(z)}$. Thus, the observed luminosity distance ($D_{L,\text{obs}}$) is related to the true luminosity distance ($D_{L,\text{true}}$) by

$$D_{L,\text{obs}} = D_{L,\text{true}} e^{\frac{\tau(z)}{2}}. \quad (1)$$

The observed distance modulus is then given by

$$\mu_{\text{obs}}(z) = \mu_{\text{true}}(z) + 2.5 (\log_{10} e) \tau(z). \quad (2)$$

In order to use the full redshift range of the available data, we adopt the following simple parametrization for a deviation from the CDD relation (Avgoustidis et al. 2009)

$$D_{L,\text{obs}} = D_A (1+z)^{2+\kappa}, \quad (3)$$

where the parameter κ reflects the degree of departure from transparency. Combining Equations (1) and (3) we obtain the exact form of the opacity depth,

$$\tau(z) = 2\kappa \ln(1+z). \quad (4)$$

To better understand the physical meaning of a constraint on κ , Avgoustidis et al. (2009) noted that for small κ and $z \leq 1$ Equation (4) is equivalent to adopting an optical depth parametrization $\tau(z) = 2\kappa z$ or $\tau(z) = (1+z)^\alpha - 1$ with the correspondence $\alpha = 2\kappa$. While this identification is based on a Taylor expansion, Avgoustidis et al. (2009) proved that the expansion is good to better than 20% for the entire κ range and the redshift range considered.

In this work, we consider the largest SN Ia sample called Pantheon, which consists of 1048 SNe Ia in the redshift range $0.01 < z < 2.3$ (Scolnic et al. 2018). The observed distance

moduli of SNe can be calculated from the SALT2 light-curve fit parameters using the formula

$$\mu_{\text{obs}}^{\text{SN}} = m_B - M_B + \alpha x_1 - \beta C + \Delta_M + \Delta_B, \quad (5)$$

where m_B is the observed B -band apparent magnitude, M_B is the absolute B -band magnitude, x_1 and C are, respectively, the light-curve stretch factor and color parameter, Δ_M denotes a distance correction based on the host galaxy mass, and Δ_B represents a distance correction from various biases predicted from simulations. α and β are nuisance parameters that describe the luminosity–stretch and luminosity–color relations.

Generally, the two nuisance parameters α and β are determined by fitting simultaneously with cosmological parameters in a specific cosmological model. In this sense, the derived distances of SNe Ia are cosmological-model-dependent. To avoid this problem, [Kessler & Scolnic \(2017\)](#) introduced the BEAMS with Bias Corrections (BBC) method to calibrated the SNe. This method relies heavily on [Marriner et al. \(2011\)](#) but involves extensive simulations to correct the SALT2 fit parameters m_B , x_1 , and C . The BBC fit creates a bin-averaged Hubble diagram from SN Ia data, and then the nuisance parameters α and β are determined by fitting to an arbitrary cosmological model, which is referred as the reference cosmology. The reference cosmological model is required to well describe the local shape of the Hubble diagram within each redshift bin. As long as the number of bins is large enough, the fitted parameters α and β will converge to consistent values, which are independent of the reference cosmology ([Marriner et al. 2011](#)).

The distances of the Pantheon SNe were calibrated after using SALT2 light-curve fitter, then applying the BBC method to determine the nuisance parameters, and adding the distance bias corrections ([Scolnic et al. 2018](#)). The corrected apparent magnitudes $m_{\text{corr}} = \mu_{\text{obs}}^{\text{SN}} + M_B$ of the Pantheon data are reported in [Scolnic et al. \(2018\)](#). Therefore, to obtain the observed distance modulus $\mu_{\text{obs}}^{\text{SN}}$, we just need to subtract M_B from m_{corr} and no longer need to do the stretch and color corrections. Considering the effect of cosmic opacity on standard candles, the true distance modulus can be written as

$$\mu_{\text{true}}^{\text{SN}}(z) = m_{\text{corr}} - M_B - 5\kappa \log_{10}(1+z), \quad (6)$$

where we emphasize that κ and M_B are the only two free parameters.

3. GW STANDARD SIRENS

From the observations of GW signals, caused by the coalescence of compact binaries, one can obtain an absolute measure of D_L . If compact binaries are black hole (BH)–NS or NS–NS binaries, the source redshifts may be available from EM counterparts that associated with the GW events

([Nissanke et al. 2010](#); [Sathyaprakash et al. 2010](#); [Zhao et al. 2011](#); [Cai & Yang 2017](#)). Therefore, this offers a model-independent way to establish the D_L – z relation (or the Hubble diagram) over a wide redshift range. The ET, with the designed high-sensitivity (10 times more sensitive in amplitude than current advanced laser interferometric detectors) and wide frequency range ($1 - 10^4$ Hz), would be able to see NS–NS merger GW events up to redshifts of $z \sim 2$ and BH–NS events up to $z > 2$ ([Punturo et al. 2010](#)). In this section, we briefly summarize the method to simulate the GW data from the ET.

The first step for generating GW standard sirens is to simulate the redshift distribution of the sources. Following [Zhao et al. \(2011\)](#) and [Cai & Yang \(2017\)](#), we expect the source redshifts can be measured by identifying EM counterparts from the coalescence of double NSs and BH–NS binaries. The redshift distribution of the observable sources takes the form ([Zhao et al. 2011](#))

$$P(z) \propto \frac{4\pi D_C^2(z) R(z)}{H(z)(1+z)}, \quad (7)$$

where $D_C(z)$ denotes the comoving distance and $R(z)$ is the merger rate of binary systems (BH–NS or NS–NS) with the expression ([Schneider et al. 2001](#); [Cutler & Holz 2009](#))

$$R(z) = \begin{cases} 1+2z, & z \leq 1 \\ \frac{3}{4}(5-z), & 1 < z < 5 \\ 0, & z \geq 5. \end{cases} \quad (8)$$

We simulate the source redshift z according to this redshift distribution. Note that although the Pantheon sample covers a wide redshift range of $0.01 < z < 2.3$, there is only one SN located at $z > 2$ ([Scolnic et al. 2018](#)). To be consistent with the redshift range of the Pantheon SNe, we consider the potential observations of GW events in $0 < z < 2.0$. With the mock z , the fiducial luminosity distance D_L^{fid} can be calculated in the fiducial flat Λ CDM model

$$D_L(z) = \frac{1+z}{H_0} \int_0^z \frac{dz}{\sqrt{\Omega_m(1+z)^3 + 1 - \Omega_m}}. \quad (9)$$

Here we adopt the following cosmological parameters: $H_0 = 70.0 \text{ km s}^{-1} \text{ Mpc}^{-1}$ and $\Omega_m = 0.298$ ([Scolnic et al. 2018](#)).

The next step is to get the total error σ_{D_L} in the luminosity distance of the GW source. In order to calculate σ_{D_L} , one needs to generate the waveform of GWs. The detector response to a GW signal is a linear combination of two wave polarizations, $h(t) = F_+ h_+(t) + F_\times h_\times(t)$. The detector’s antenna pattern functions F_+ and F_\times depend on the source’s position (θ_s, ϕ_s) and the polarization angle ψ_s . The restricted post-Newtonian approximation waveforms h_\times and h_+ for the non-spinning compact binaries depend on the symmetric mass ratio $\eta = m_1 m_2 / (m_1 + m_2)^2$, the chirp mass $\mathcal{M}_c =$

$(m_1 + m_2)\eta^{3/5}$ (m_1 and m_2 are component masses of a coalescing binary), the inclination angle ι between the binary's orbital and the line-of-sight, the D_L , the epoch of the merger t_0 , and the merging phase ψ_0 (Sathyaprakash & Schutz 2009). So, for a given binary, the response of the detector depends on $(\mathcal{M}_c, \eta, t_0, \psi_0, \theta_s, \phi_s, \psi_s, \iota, D_L)$. Using the Fisher information matrix and marginalizing over the other parameters, we can estimate the instrumental error $\sigma_{D_L}^{\text{inst}}$ on the measurement of D_L . In addition to $\sigma_{D_L}^{\text{inst}}$, we also consider an error $\sigma_{D_L}^{\text{lens}}/D_L = 0.05z$ due to the weak lensing effect. Thus, the total uncertainty is $\sigma_{D_L} = [(\sigma_{D_L}^{\text{inst}})^2 + (\sigma_{D_L}^{\text{lens}})^2]^{1/2}$. Readers may refer to Cai & Yang (2017) for detailed information about the production of σ_{D_L} (see also Zhao et al. 2011; Wang et al. 2018; Wei et al. 2018; Wei 2018). Note that the signal is identified as a GW detection only when the evaluated signal-to-noise ratio (S/N) is larger than 8.0. For every confirmed detection (i.e., $S/N > 8.0$), the fiducial luminosity distance D_L^{fid} is converted to the fiducial distance modulus by

$$\mu^{\text{fid}} = 5 \log_{10} \left(\frac{D_L^{\text{fid}}}{\text{Mpc}} \right) + 25, \quad (10)$$

and the error of μ^{fid} is propagated from that of D_L^{fid} by

$$\sigma_{\mu^{\text{GW}}} = \frac{5}{\ln 10} \frac{\sigma_{D_L}}{D_L^{\text{fid}}}. \quad (11)$$

We then add the deviation $\sigma_{\mu^{\text{GW}}}$ to the fiducial value of μ^{fid} . That is, we sample the μ^{GW} measurement according to the Gaussian distribution $\mu^{\text{GW}} = \mathcal{N}(\mu^{\text{fid}}, \sigma_{\mu^{\text{GW}}})$.

Using the method described above, one can generate a catalog of the simulated GW events with z , μ^{GW} , and $\sigma_{\mu^{\text{GW}}}$. As argued in Cai & Yang (2017), the ET is expected to detect $\mathcal{O}(10^2)$ GW sources with EM counterparts per year. Thus, we first simulate a population of 100 such events. An example of 100 simulated GW data (blue dots)¹ from the fiducial model is presented in Figure 1.

4. UNBIASED CONSTRAINTS ON COSMIC OPACITY

Future detectable GW sources are expected to distribute in nearly the same redshift range as the SN Ia data, and the opacity-free μ^{GW} of GW events can be provided by the GW observations alone. By confronting distance moduli $\mu^{\text{GW}}(z)$ from the simulated GW events with distance moduli $\mu_{\text{true}}^{\text{SN}}(z)$ in Equation (6) that depend on κ and M_B from observations of SNe Ia at the same redshifts, we can obtain a model-independent constraint on cosmic opacity. However, in reality, it is difficult to have both μ^{GW} and $\mu_{\text{true}}^{\text{SN}}$ at exactly the same redshift. So, as Holanda et al. (2010) and Li et al. (2011) did in their treatments, we find the nearest redshift to GW data from SNe Ia and use the criteria ($\Delta z = |z_{\text{GW}} - z_{\text{SN}}| < 0.005$) to ensure the redshift differences of the nearest SNe Ia to GW data are not too large. For the

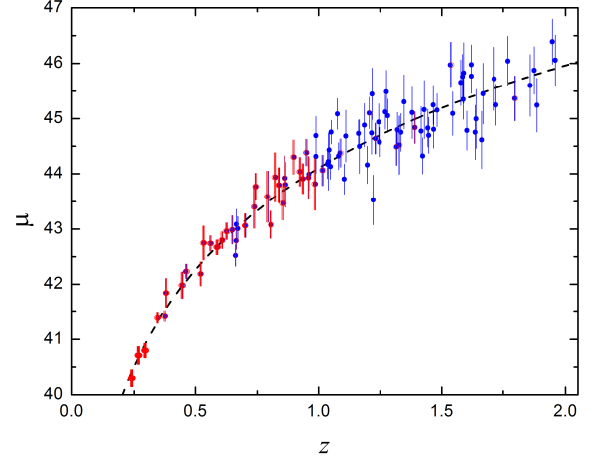


Figure 1. Example catalog of 100 simulated GW events (blue dots) with redshifts z , distance moduli μ , and the errors in the distance moduli σ_{μ} . The dashed line is the fiducial flat Λ CDM model. Red circles represent 213 Pantheon SNe Ia whose distance moduli are determined by the nearest GW data, other 835 SNe Ia that have redshift differences $\Delta z \geq 0.005$ with respect to their corresponding nearest GW data are discarded.

example of 100 simulated GW data shown in Figure 1, we find that there are 213 Pantheon SNe Ia (red circles) that satisfy the redshift selection criteria. Other 835 SNe Ia that have redshift differences $\Delta z \geq 0.005$ are discarded.

We now give the χ^2 statistic for constraining cosmic opacity parameterized by κ ,

$$\chi^2(\kappa, M_B) = \sum_i \frac{[\mu_{\text{true}}^{\text{SN}}(z_i; \kappa, M_B) - \mu^{\text{GW}}(z_i)]^2}{\sigma_{\mu^{\text{SN},i}}^2 + \sigma_{\mu^{\text{GW},i}}^2}, \quad (12)$$

where $\sigma_{\mu^{\text{SN}}}$ is the observational error of the SN distance modulus. Here only the statistical uncertainties are considered since only part of Pantheon SNe Ia are selected to match the simulated GW data. To make sure the final constraints are unbiased, we repeat this process 1000 times for each GW data set using different noise seeds. Figure 2 displays the constraint results on κ and M_B . We find that, from 100 simulated GW events and observations of Pantheon SNe Ia, the unbiased constraint on cosmic opacity is $\kappa = 0.009 \pm 0.046$ (1σ).¹

Note that the number of observable GW events is quite uncertain. To test how the uncertainty of κ depends on the number of simulated GW events (N_{GW}), in Figure 3 and Table 1 we show the best-fit κ and 1σ confidence level as a function of N_{GW} . One can see from Figure 3 and Table 1 that the uncertainty of κ is gradually reduced with the increasing of the number of GW events, finally turns to a relatively sta-

¹ After this work appeared on arXiv, we found a similar work (Qi et al. 2019), which has also independently investigated opacity constraints from GWs and SNe Ia.

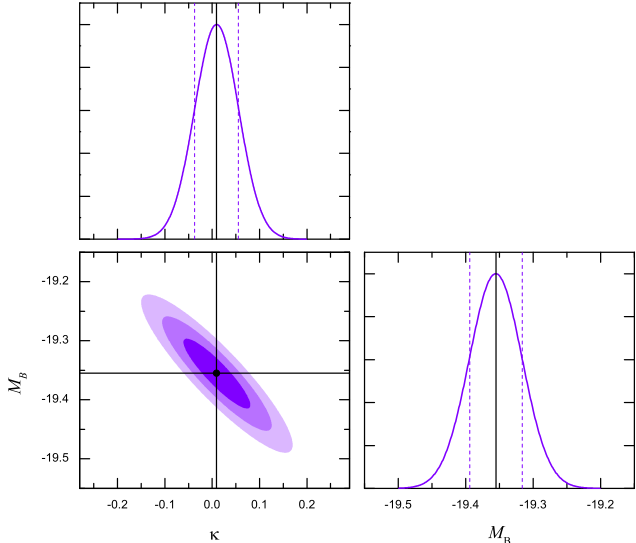


Figure 2. 1-D marginalized probability distributions and 1–3 σ constraint contours for cosmic opacity κ and SN Ia absolute magnitude M_B , using 100 simulated GW events and observations of Pantheon SNe Ia. The vertical solid lines represent the best-fit values, and the vertical dashed lines enclose the 1 σ credible region.

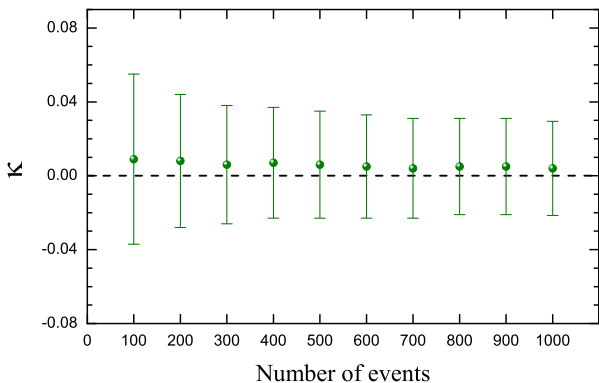


Figure 3. Best-fit cosmic opacity κ and 1 σ confidence level as a function of the number of GW events. The dashed line corresponds to a transparent universe.

ble value (i.e., $\sigma_\kappa \simeq 0.026$). The constraint results are nearly the same for the cases of $N_{\text{GW}} \geq 800$, which is understandable. We only use the data of GWs and SNe Ia that satisfying the criteria ($\Delta z = |z_{\text{GW}} - z_{\text{SN}}| < 0.005$) to constrain κ . With the fixed Pantheon SN sample ($N_{\text{SN}} = 1048$), the number of GW/SN pairs satisfying the redshift selection criteria would begin to stabilize and the resulting constraints would be nearly the same, when the number of GW events is large enough.

By the time we have ET results, much more SN Ia data with wider redshift range may be detected by future SN surveys. It is expected that more than 2000 SNe Ia can be de-

Table 1. Summary of Unbiased Cosmic Opacity Constraints from N_{GW} Simulated GW Events and Observations of Pantheon SNe Ia

N_{GW}	κ	N_{GW}	κ
100	0.009 ± 0.046	600	0.005 ± 0.028
200	0.008 ± 0.036	700	0.004 ± 0.027
300	0.006 ± 0.032	800	0.005 ± 0.026
400	0.007 ± 0.030	900	0.005 ± 0.026
500	0.006 ± 0.029	1000	0.004 ± 0.026

tected in the era of the *Wide Field Infrared Survey Telescope* (*WFIRST*) (Green et al. 2012). To better represent how effective our method might be with more SN Ia measurements, we also perform Monte Carlo simulations to create the mock $\mu_{\text{obs}}^{\text{SN}} - z$ data sets. We assume that there are 2000 SNe Ia by the time that 1000 GW events are detected. The redshift distribution of SNe Ia is adopted as

$$P_{\text{SN}}(z) \propto \frac{4\pi D_C^2(z) R_{\text{SN}}(z)}{H(z)(1+z)}, \quad (13)$$

where $R_{\text{SN}}(z)$ is the volumetric rate of SNe Ia, which is given by (Hounsell et al. 2018)

$$R_{\text{SN}}(z) = \begin{cases} 2.5 \times (1+z)^{1.5} (10^{-5} \text{ Mpc}^{-3} \text{ yr}^{-1}), & \text{for } z \leq 1 \\ 5.0 \times (1+z)^{0.5} (10^{-5} \text{ Mpc}^{-3} \text{ yr}^{-1}), & \text{for } 1 < z < 3. \end{cases} \quad (14)$$

As the expected detection rate for $z > 3$ SNe is low, we do not attempt to simulate SNe at those redshifts. Following Hounsell et al. (2018), the total distance uncertainty $\sigma_{\mu^{\text{SN}}}$ of each mock SN is calculated by the sum of the systematic uncertainty σ_{sys} and the statistical uncertainty σ_{stat} , i.e., $\sigma_{\mu^{\text{SN}}}^2 = \sigma_{\text{sys}}^2 + \sigma_{\text{stat}}^2$. The systematic uncertainty is assumed to increase with redshift, $\sigma_{\text{sys}} = \frac{0.01(1+z)}{1.8}$ (mag). The statistical uncertainty is $\sigma_{\text{stat}}^2 = \sigma_{\text{meas}}^2 + \sigma_{\text{int}}^2 + \sigma_{\text{lens}}^2$, where $\sigma_{\text{meas}} = 0.08$ mag includes both statistical measurement uncertainties and statistical model uncertainties, $\sigma_{\text{int}} = 0.09$ mag denotes the intrinsic scatter in the corrected SN Ia distances, and $\sigma_{\text{lens}} = 0.07 \times z$ mag represents the lensing uncertainty. The route of GW simulation is the same as described earlier in Section 3, but now we consider the potential observations of GW events in $0 < z < 3.0$. Figure 4 gives an example of the simulations for the case of 2000 simulated SNe Ia and 1000 simulated GW events. From top to bottom, the three panels show the Hubble diagram of 2000 simulated SNe Ia with the fiducial flat Λ CDM model (dashed line), the Hubble diagram of 1000 simulated GW events with the fiducial flat Λ CDM model (dashed line), and the final constraint on κ , respectively. In this case, the final derived κ is $\kappa = 0.0000 \pm 0.0044$ (1 σ). Compared with the constraint obtained from 1048 Pantheon SNe Ia and 800 simulated GW events ($\kappa = 0.005 \pm 0.026$), the uncertainty of the determined κ in this case can be further improved by a factor of ~ 6.0 .

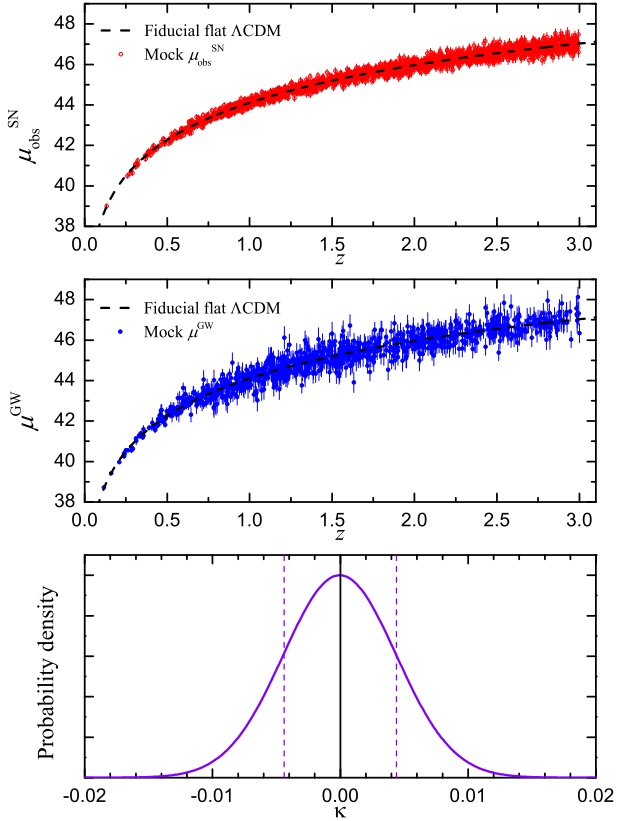


Figure 4. An example of the simulations for the case of 2000 simulated SNe Ia and 1000 simulated GW events. Top panel shows the Hubble diagram of 2000 simulated SNe Ia with the fiducial flat Λ CDM model (dashed line). Middle panel shows the Hubble diagram of 1000 simulated GW events with the fiducial flat Λ CDM model (dashed line). Bottom panel shows the final constraint on cosmic opacity κ from these data.

In our above simulations, the fiducial model is chosen to be flat Λ CDM. To investigate a possible degeneracy of the results with the adopted fiducial model, we also consider two separate cosmological models: w CDM and non-flat Λ CDM. We take the best-fit cosmological parameters from the Pantheon SN sample (Scolnic et al. 2018) as the fiducial models (w CDM: $\Omega_m = 0.316$ and $w = -1.09$; nonflat Λ CDM: $\Omega_m = 0.319$ and $\Omega_\Lambda = 0.733$) to generate 2000 simulated SNe Ia and 1000 simulated GW events in $0 < z < 3.0$. The final opacity constraints are $\kappa = -0.0003 \pm 0.0044$ and $\kappa = -0.0004 \pm 0.0044$ for the fiducial w CDM and nonflat Λ CDM models, respectively. By comparing these constraints with that obtained from the fiducial flat Λ CDM model ($\kappa = 0.0000 \pm 0.0044$), we can conclude that the opacity constraints are independent of the adopted fiducial model.

5. SUMMARY AND DISCUSSION

Cosmic opacity may be due to absorption or scattering caused by dust in the universe, or may result from other exotic mechanisms where extragalactic magnetic fields turn

photons into unobserved particles (e.g., light axions, gravitons, chameleons, Kaluza-Klein modes). The presence of cosmic opacity can lead to a significant deviation from photon number conservation, thus making the observed SNe Ia dimmer than what expected and affecting the reliable reconstruction of the cosmic expansion history. It is therefore crucial to quantitatively study the effect of cosmic opacity on SN standard candles.

As the luminosity distances of GWs can be directly obtained from their waveform signals rather than from luminosities, they are independent of the non-conservation of photon number and thus are not affected by cosmic opacity. In this work, we first propose that combining the GW observations with SN Ia data in similar redshift ranges provides a novel way to constrain cosmic opacity. Unbiased cosmic opacity constraints are performed by comparing two kinds of distance moduli obtained from the recent Pantheon compilation of SN Ia data and future GW observations of the ET. Our simulations show that, from 1048 SN Ia measurements and 100 simulated GW events, the cosmic opacity parameter κ is expected to be constrained with an accuracy of $\sigma_\kappa \sim 0.046$. If 800 GW events are observed, the uncertainty of κ can be further reduced to ~ 0.026 . We also demonstrate that with 2000 simulated SNe Ia and 1000 simulated GW events, one can expect the transparent universe to be estimated at the precision of $\kappa = 0.0000 \pm 0.0044$.

Previously, Avgoustidis et al. (2009, 2010) obtained $\kappa = -0.01^{+0.08}_{-0.09}$ and $\kappa = -0.04^{+0.08}_{-0.07}$ by analyzing SN Ia and $H(z)$ data in the flat Λ CDM model. From the joint analyses involving gamma-ray bursts and $H(z)$ measurements, Holanda & Busti (2014) obtained $\kappa = 0.06^{+0.18}_{-0.18}$ and $\kappa = 0.057^{+0.21}_{-0.21}$ in the flat Λ CDM and XCDM frameworks, respectively. Liao et al. (2015) obtained a model-independent constraint on cosmic opacity ($\kappa = 0.07^{+0.11}_{-0.12}$) by comparing the distances from SN Ia and $H(z)$ observations. Jesus et al. (2017) tested the conservation of photon number with distances from SNe Ia and those inferred from ages of 32 old objects, yielding $\kappa = -0.18^{+0.25}_{-0.24}$. By comparing our results with previous opacity constraints involving distances from different observations, we prove that our method using GW standard sirens and SN Ia standard candles will be competitive. Most importantly, our method offers a new model-independent way to constrain cosmic opacity.

We are grateful to the anonymous referee for helpful comments. This work is partially supported by the National Natural Science Foundation of China (grant Nos. U1831122, 11603076, 11673068, and 11725314), the Youth Innovation Promotion Association (2017366), the Key Research Program of Frontier Sciences (grant No. QYZDB-S5W-SYS005), the Strategic Priority Research Program “Multi-waveband gravitational wave Universe” (grant No.

XDB23000000) of Chinese Academy of Sciences, and the

“333 Project” and the Natural Science Foundation (grant No. BK20161096) of Jiangsu Province.

REFERENCES

- Abbott, B. P., Abbott, R., Abbott, T. D., et al. 2017, *Nature*, 551, 85
- Aguirre, A. N. 1999a, *ApJL*, 512, L19
- Aguirre, A. 1999b, *ApJ*, 525, 583
- Avgoustidis, A., Burrage, C., Redondo, J., Verde, L., & Jimenez, R. 2010, *JCAP*, 10, 024
- Avgoustidis, A., Verde, L., & Jimenez, R. 2009, *JCAP*, 6, 012
- Bassett, B. A., & Kunz, M. 2004, *PhRvD*, 69, 101305
- Burrage, C. 2008, *PhRvD*, 77, 043009
- Cai, R.-G., Liu, T.-B., Liu, X.-W., Wang, S.-J., & Yang, T. 2018, *PhRvD*, 97, 103005
- Cai, R.-G., & Yang, T. 2017, *PhRvD*, 95, 044024
- Chen, J., Wu, P., Yu, H., & Li, Z. 2012, *JCAP*, 10, 029
- Chen, P. 1995, *Physical Review Letters*, 74, 634
- Csáki, C., Kaloper, N., & Terning, J. 2002, *Physical Review Letters*, 88, 161302
- Cutler, C., & Holz, D. E. 2009, *PhRvD*, 80, 104009
- Deffayet, C., & Uzan, J.-P. 2000, *PhRvD*, 62, 063507
- Del Pozzo, W. 2012, *PhRvD*, 86, 043011
- Del Pozzo, W., Li, T. G. F., & Messenger, C. 2017, *PhRvD*, 95, 043502
- Du, M., Yang, W., Xu, L., Pan, S., & Mota, D. F. 2018, *arXiv e-prints*, arXiv:1812.01440
- Ellis, G. F. R. 2007, *General Relativity and Gravitation*, 39, 1047
- Ellis, G. F. R., Poltis, R., Uzan, J.-P., & Weltman, A. 2013, *PhRvD*, 87, 103530
- Etherington, I. M. H. 1933, *Philosophical Magazine*, 15
- Gonçalves, R. S., Holanda, R. F. L., & Alcaniz, J. S. 2012, *MNRAS*, 420, L43
- Green, J., Schechter, P., Baltay, C., et al. 2012, *arXiv e-prints*, arXiv:1208.4012
- Holanda, R. F. L., & Busti, V. C. 2014, *PhRvD*, 89, 103517
- Holanda, R. F. L., Carvalho, J. C., & Alcaniz, J. S. 2013, *JCAP*, 4, 027
- Holanda, R. F. L., Lima, J. A. S., & Ribeiro, M. B. 2010, *ApJL*, 722, L233
- Holanda, R. F. L., Lima, J. A. S., & Ribeiro, M. B. 2011, *A&A*, 528, L14
- Holanda, R. F. L., Lima, J. A. S., & Ribeiro, M. B. 2012, *A&A*, 538, A131
- Holz, D. E., & Hughes, S. A. 2005, *ApJ*, 629, 15
- Hounsell, R., Scolnic, D., Foley, R. J., et al. 2018, *ApJ*, 867, 23
- Hu, J., & Wang, F. Y. 2018, *MNRAS*, 477, 5064
- Hu, J., Yu, H., & Wang, F. Y. 2017, *ApJ*, 836, 107
- Jaeckel, J., & Ringwald, A. 2010, *Annual Review of Nuclear and Particle Science*, 60, 405
- Jesus, J. F., Holanda, R. F. L., & Dantas, M. A. 2017, *General Relativity and Gravitation*, 49, 150
- Kessler, R., & Scolnic, D. 2017, *ApJ*, 836, 56
- Khedekar, S., & Chakraborti, S. 2011, *Physical Review Letters*, 106, 221301
- Khoury, J., & Weltman, A. 2004, *Physical Review Letters*, 93, 171104
- Li, Z., Wu, P., & Yu, H. 2011, *ApJL*, 729, L14
- Li, Z., Wu, P., Yu, H., & Zhu, Z.-H. 2013, *PhRvD*, 87, 103013
- Liao, K., Avgoustidis, A., & Li, Z. 2015, *PhRvD*, 92, 123539
- Liao, K., Li, Z., Cao, S., et al. 2016, *ApJ*, 822, 74
- Liao, K., Li, Z., Ming, J., & Zhu, Z.-H. 2013, *Physics Letters B*, 718, 1166
- Lima, J. A. S., Cunha, J. V., & Zanchin, V. T. 2011, *ApJL*, 742, L26
- Lin, H.-N., Li, M.-H., & Li, X. 2018a, *MNRAS*, 480, 3117
- Lin, H.-N., Li, J., & Li, X. 2018b, *European Physical Journal C*, 78, 356
- Lv, M.-Z., & Xia, J.-Q. 2016, *Physics of the Dark Universe*, 13, 139
- Ma, C., & Corasaniti, P.-S. 2018, *ApJ*, 861, 124
- Marriner, J., Bernstein, J. P., Kessler, R., et al. 2011, *ApJ*, 740, 72
- Melia, F. 2018, *MNRAS*, 481, 4855
- Meng, X.-L., Zhang, T.-J., Zhan, H., & Wang, X. 2012, *ApJ*, 745, 98
- Messenger, C., Takami, K., Gossan, S., Rezzolla, L., & Sathyaprakash, B. S. 2014, *Physical Review X*, 4, 041004
- More, S., Bovy, J., & Hogg, D. W. 2009, *ApJ*, 696, 1727
- Nair, R., Jhingan, S., & Jain, D. 2011, *JCAP*, 5, 023
- Nair, R., Jhingan, S., & Jain, D. 2012, *JCAP*, 12, 028
- Nissanke, S., Holz, D. E., Hughes, S. A., Dalal, N., & Sievers, J. L. 2010, *ApJ*, 725, 496
- Perlmutter, S., Aldering, G., Goldhaber, G., et al. 1999, *ApJ*, 517, 565
- Punturo, M., Abernathy, M., Acernese, F., & et al. 2010, *Classical and Quantum Gravity*, 27, 194002
- Qi, J.-Z., Cao, S., Pan, Y., & Li, J. 2019, *arXiv e-prints*, arXiv:1902.01702
- Rana, A., Jain, D., Mahajan, S., & Mukherjee, A. 2016, *JCAP*, 7, 026
- Riess, A. G., Filippenko, A. V., Challis, P., et al. 1998, *AJ*, 116, 1009
- Ruan, C.-Z., Melia, F., & Zhang, T.-J. 2018, *ApJ*, 866, 31
- Sathyaprakash, B. S., & Schutz, B. F. 2009, *Living Reviews in Relativity*, 12, 2

- Sathyaprakash, B. S., Schutz, B. F., & Van Den Broeck, C. 2010, *Classical and Quantum Gravity*, 27, 215006
- Schneider, R., Ferrari, V., Matarrese, S., & Portegies Zwart, S. F. 2001, *MNRAS*, 324, 797
- Schutz, B. F. 1986, *Nature*, 323, 310
- Scolnic, D. M., Jones, D. O., Rest, A., et al. 2018, *ApJ*, 859, 101
- Uzan, J.-P., Aghanim, N., & Mellier, Y. 2004, *PhRvD*, 70, 083533
- Wang, G.-J., Wei, J.-J., Li, Z.-X., Xia, J.-Q., & Zhu, Z.-H. 2017, *ApJ*, 847, 45
- Wang, L.-F., Zhang, X.-N., Zhang, J.-F., & Zhang, X. 2018, *Physics Letters B*, 782, 87
- Wei, J.-J. 2018, *ApJ*, 868, 29
- Wei, J.-J., Wu, X.-F., & Gao, H. 2018, *ApJL*, 860, L7
- Yang, T., Holanda, R. F. L., & Hu, B. 2017, arXiv e-prints, arXiv:1710.10929
- Yang, X., Yu, H.-R., Zhang, Z.-S., & Zhang, T.-J. 2013, *ApJL*, 777, L24
- Zhao, W., van den Broeck, C., Baskaran, D., & Li, T. G. F. 2011, *PhRvD*, 83, 023005
- Zhao, W., & Wen, L. 2018, *PhRvD*, 97, 064031
- Zhao, W., Wright, B. S., & Li, B. 2018, *JCAP*, 10, 052